CIT-9: a fault-free, gmelinite zeolite

Supporting Information

1. Synthesis and treatments

1.1 Synthesis and details of used OSDAs

N,N-dimethyl-3,5-dimethylpiperidinium hydroxide

Different mixtures of cis and trans isomers of N,N-dimethyl-3,5-dimethylpiperidinium were acquired from SACHEM in their hydroxide forms. Full synthetic details of these organic compounds can be found in our previous work.[1] A 'pure cis' mixture with a 98/2 (cis/trans) isomer distribution, as well as a nearly 'racemic' 48/52 mixture was used.

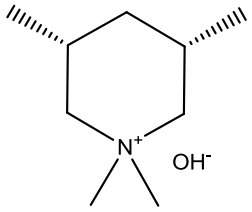

Synthesis of Dab-4-Br polymer

Dab-4-Br polymer was prepared as previously reported.[2] As a typical synthesis process, 16.8 g of 1,4-diazabicyclo[2.2.2]octane (150 mmol, Sigma-Aldrich, 98%) was mixed with 250 ml of dimethyl sulfoxide (DMSO), and the mixture was heated up to 45°C. While violently stirring, 32.4 g of 1,4-dibromobutane (150 mmol, Sigma-Aldrich, 99%) was gradually added dropwise over 30 min. After 1 hour of mixing, the reaction mixture was heated to 110°C and maintained for 6 hours. And then, the mixture was slowly cooled down to room temperature. The solid was filtrated and washed with a copious amount (4 L) of diethyl ether repeatedly. The bright-yellowish product was dried in a vacuum chamber for 24 hours at room temperature.

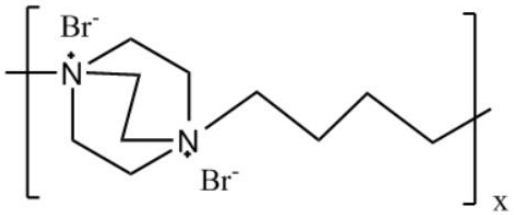

1.2 Synthesis of Microporous materials

Synthesis of CIT-9 GME

Typical gels for crystallizing pure CIT-9 GME phases were prepared by mixing sodium silicate (PQ, Waterglass N®; composition: 8.9 wt% Na_2O-28.7 wt% SiO_2-62.4 wt% H_2O, Na_2O/SiO_2 molar ratio of 3.22), USY CBV500 (Zeolyst, SiO_2/Al_2O_3 = 5.2), aqueous solution of tetramethyl-N,N,3,5-piperidinium hydroxide (SACHEM, 98% cis/2% trans), 1 M NaOH aqueous solution (Sigma-Aldrich), and distilled water. The desired final gel composition was 1.0 SiO_2 : x Al_2O_3 : 0.18 ROH : 0.53 NaOH : 20.4 H_2O where x = 0.0278-0.0417 preferably. CIT-9 samples from gels of x = 0.0333 (SiO_2/Al_2O_3 30 or Si/Al 15) were chosen as *the representative CIT-9* studied and characterized in most part of this article. Different Si-source (*e.g.*, fumed silica) could be also used to achieve the desired gel compositions

instead of sodium silicate. The mixture was charged into a 23 ml Parr PTFE-lined autoclave and stirred for 24 hours at room temperature (not critical it seemed). After 24 hours of digestion, the autoclave was sealed and placed in a 140°C tumbling oven, and the crystallization was conducted for 36-110 hours (preferably 110 hours). Static syntheses usually also work. The solids were separated by centrifugation and/or filtration (scale dependent) and washed with water, methanol and acetone, and dried at 70°C.

Synthesis of dabco-GME

Dabco-GME was synthesized as previously mentioned in literature.[3] As a typical procedure, colloidal silica aqueous dispersion (Sigma-Aldrich, Ludox® HS-30), sodium aluminate (Alfa Aesar, 37.9 wt% Na_2O-51.1 wt% Al_2O_3-11.0 wt% H_2O), Dab-4-Br polymer, sodium hydroxide (Mallinckrodt chemicals, 98.8%) and distilled water were mixed in a 45 ml Parr PTFE-lined autoclave and vigorously stirred for 24 hours at room temperature. The desired final gel composition was 1.0 SiO_2 : 0.033 Al_2O_3 : 1.2 NaOH : 0.24 R : 44.0 H_2O. After the complete dissolution, the autoclave was sealed and placed in a 90°C static oven. After 22 days of crystallization, the solid product was recovered by filtration, and rinsed thoroughly with distilled water, methanol and acetone, and dried in a convection oven at 70°C.

Sr-GME and Natural gmelinite samples

Natural gmelinite originated from Cairns Bay Flinder's Shire, Victoria, Australia. The Sr-GME sample was made and described by Chiyoda et al.[4] More details in that work on both materials.

1.3 Ozone treatment and preparation of K-exchanged GME

As-prepared GME was treated under an ozone/oxygen flow (26 μg O_3/cc O_2) at 150°C for 24 hours to remove organic compounds. Freshly ozone-treated GME zeolite was mixed with 1 M KCl solution and heated up to 85°C and stirred for cation exchange. (solid : liquid = 1 mg : 1 ml) After 1 day, the solid was recovered by filtration, and the same procedure of cation exchange was repeated twice more. Finally, excess KCl salt was thoroughly washed with warm distilled water. The final calcination was performed in dry flowing air (20 ml min^{-1}) by heating to 150 °C at 1 °C·min^{-1}; holding for 3 h at 150 °C, and then heating further to 580 °C at 1 °C·min^{-1} and held for 6 h.

1.4. Preparation of K-salt-mixed-calcined GME

The K-salt-mixed-calcined GME sample series were prepared according to the method reported in a patent for dabco-GME.[5] As-prepared GME was mixed with 2 mol kg^{-1} KCl solution. (solid : liquid = 1 mg : 2.1 mg) NaCl solution or NaCl-KCl mixed solution could be used instead of KCl solution. The resulting thick paste was aged for 6 hours at room temperature, and placed in a muffle furnace. A slow calcination was performed under a dry air flow (20 ml min^{-1}) by ramping the temperature from room temperature to 90°C at 0.1°C min^{-1}, 90°C to 500°C at 0.5°C min^{-1}, and finally staying at 500°C for 5 hours. The resulting material was thoroughly washed with warm distilled water to remove excess salt. The second calcination was performed at 580°C as described under 1.3.

1.5. Steaming of K-exchanged CIT-9 GME

The steaming treatments of K-form CIT-9 GME were performed under the atmospheric pressure as mentioned in our previous reports.[6] Briefly, 200-500 mg of K-exchanged CIT-9 GME was loaded in the ceramic calcination boats, and placed the middle of the 3" tube of an MTI OTF-1200X tube furnace. The furnace temperature was slowly ramped up to 600-700 °C, and a flow of zero-grade air saturated with water vapor (bubbler temperature = 60-80 °C, corresponding to steam partial pressures of 20-47 kPa) was fed throughout heating treatments at 50 cc min^{-1}. The results of steaming study were provided in Section 3.17 of this Supporting Information.

2. Characterization

2.1 XRD, MAS NMR, TGA, SEM/EDS

Powder X-ray diffraction (XRD) profiles were collected on a Rigaku MiniFlex II diffractometer with Cu Kα radiation (λ = 0.15418 nm). Solid-state magic-angle spinning (MAS) nuclear magnetic resonance (NMR) experiments were conducted using a Bruker Avance 500 MHz spectrometer with an 11.2 T Bruker UltraShield magnet. Zeolite powder samples were packed in a 4 mm zirconia rotor capped with a Kel-F drive cap to collect NMR spectra. The ^{13}C, ^{27}Al and ^{29}Si NMR spectra were acquired with the carrier frequencies 125 MHz (8 kHz MAS), 130 MHz (12 kHz MAS) and 99 MHz (8 kHz MAS), respectively. One Al-NMR (Fig. S19) was acquired on a 300 MHz Bruker, at 78.2 MHz of carrier frequency. Thermogravimetric analysis (TGA) profiles were collected using a PerkinElmer STA 6000 instrument with alumina crucibles under a dry nitrogen flow (19-20 ml min^{-1}) from 30°C to 900°C with a ramping rate 10°C min^{-1}. Scanning electron microgram (SEM) images were recorded using a ZEISS 1550VP field emission (FE) SEM equipped with an Oxford X-Max SDD X-ray Energy Dispersive Spectrometer (EDX) system, and the elemental analyses were performed using this EDX system.

2.2 Pore Volumes

All N_2 adsorption isotherms were measured at −196 °C on a Micromeritics Tristar II machine. Prior to analysis, the samples were outgassed under mild N2-flow at 200 °C overnight. The t-plot method was used to calculate the micropore volumes on the adsorption branch.

2.3 Molecular modelling calculations (molecular mechanics simulations)

The location and the van der Waals (vdW) interaction energy of the OSDA within the GME framework were studied by molecular mechanics simulations using the Materials Studio 6 software.(15) The CVFF force field(16) was selected for the calculation, and the most stable locations for the OSDA molecules were obtained by simulated annealing. The zeolite framework was assumed to be pure silicate, because the distribution of the Al atoms in the framework is not clear. We limited the modeling strictly to vdW interaction energies between the OSDAs and the framework and did not include inorganic cations and water molecules to the calculation. The unit cell and the framework atoms were fixed during the calculation, and in this case, a supercell was generated to better evaluate the optimum loading of the OSDA molecules in the one-dimensional 12-membered ring channel. The geometry of the OSDA molecule was first optimized using the CVFF force field and then allowed to change after it was docked to the zeolite framework. Initially, one OSDA molecule was docked per unit cell, the number was increased to three OSDA molecules per 2 unit cells (i.e., on average 1.5 OSDA molecules per unit cell), then to two per unit cell and five per 2 unit cells. The simulation results indicated that the most stable situation was when one unit cell was occupied by two OSDA molecules (Fig. S5). For the cis- tetramethyl-N,N,3,5-piperidinium hydroxide OSDA isomer this amounts to 10.7 kJ/mol (VdW energy per T-atom). Respectively -8.1 and -5.1 kJ/mol were obtained for 1.5 and 1 cis-OSDA per unit cell.

2.4 Variable Temperature XRD

Variable temperature Powder X-ray diffraction (PXRD) patterns were collected from 30 °C to 580 °C with increments of 50 °C under ambient conditions, using a PANalytical Empyrean powder diffractometer (Cu Kα radiation) equipped with an Anton Paar HTK 1200N high-temperature chamber. The sample was stabilized at each measurement temperature for 15 min before starting each measurement. The temperature ramp between two consecutive temperatures was 5 °C min^{-1}.

2.5 Rotation electron diffraction (RED)

Three-dimensional electron diffraction data were collected using the rotation electron diffraction (RED) technique.[7] On a JEOL 2010 microscope operating at 200 kV, with RED software installed, data were collected over a tilt range of ±50° with a tilt step of 0.50°. The exposure time is 3 seconds per tilt step. Streaking along certain axes indicates faulting and/or disorder. The natural gmelinite sample was not assessed with RED, as it was highly faulted (CHA intergrowth reflection in PXRD) and electron diffraction with heavy streaks of this sample was documented by Chiyoda and Davis.[4] Multiple crystals were measured and each in multiple directions. No faulting was ever observed for CIT-9.

3. Supporting Data and Figures

3.1 Synthesis remarks

A careful selection of gel composition is very essential to obtain high-purity CIT-9 **GME** crystals having high Si/Al ratios. We have tested various gel compositions focusing on the aluminum contents, the concentration of OSDA, and the water contents. It was found that CIT-9 products of the best quality were obtained by crystallizing the gel (1.0 SiO_2 : 30^{-1}-36^{-1} Al_2O_3 : 0.18-0.24 ROH : 0.53 NaOH : 20.4 H_2O) at 140°C for 96-110 hours. Increasing water content, increasing Si/Al ratio and decreasing OSDA concentration led to the formation of a competing phase **AEI**.

3.2 Effects of gel compositions on product phases during synthesis

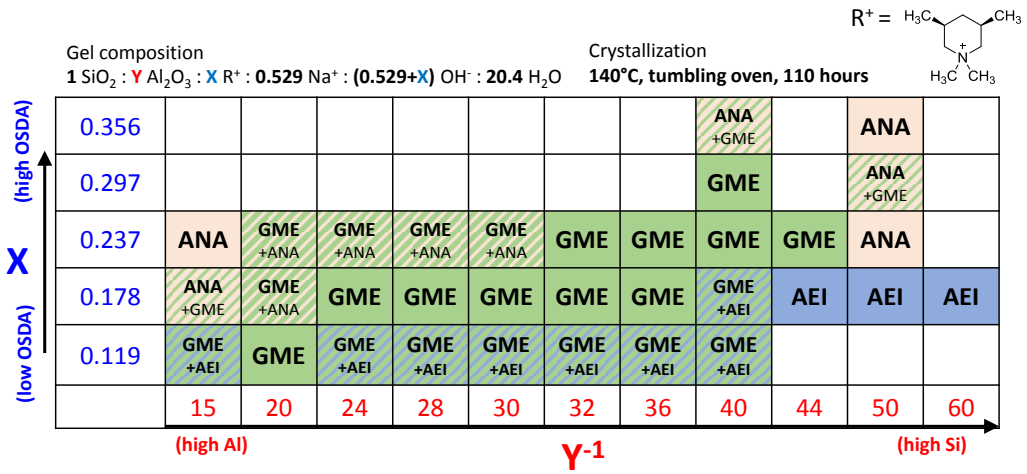

Fig. S1. The summary of the results of the systematic syntheses using N,N-dimethyl-3,5-dimethylpiperidinium OSDA.

The influences of the concentration of aluminum and that of OSDA in the gels on the product phases were studied. The crystallizations of 33 gel compositions were tested in total at 140°C. The purest CIT-9 **GME** phase was obtained when the gel composition was 1 SiO_2 : 1/30 Al_2O_3 : 0.178 ROH : 0.529 NaOH : 20.4 H_2O. The major competing phases were analcime (**ANA**) and SSZ-39 (**AEI**). The increase of the OSDA concentration and/or the aluminum concentration resulted in the increase in the amount of **ANA** impurity. On the other hand, the lower aluminum contents and/or OSDA contents tend to lead the system to crystallize the **AEI** phase. The CIT-9 **GME** phase was achieved only in the middle region.

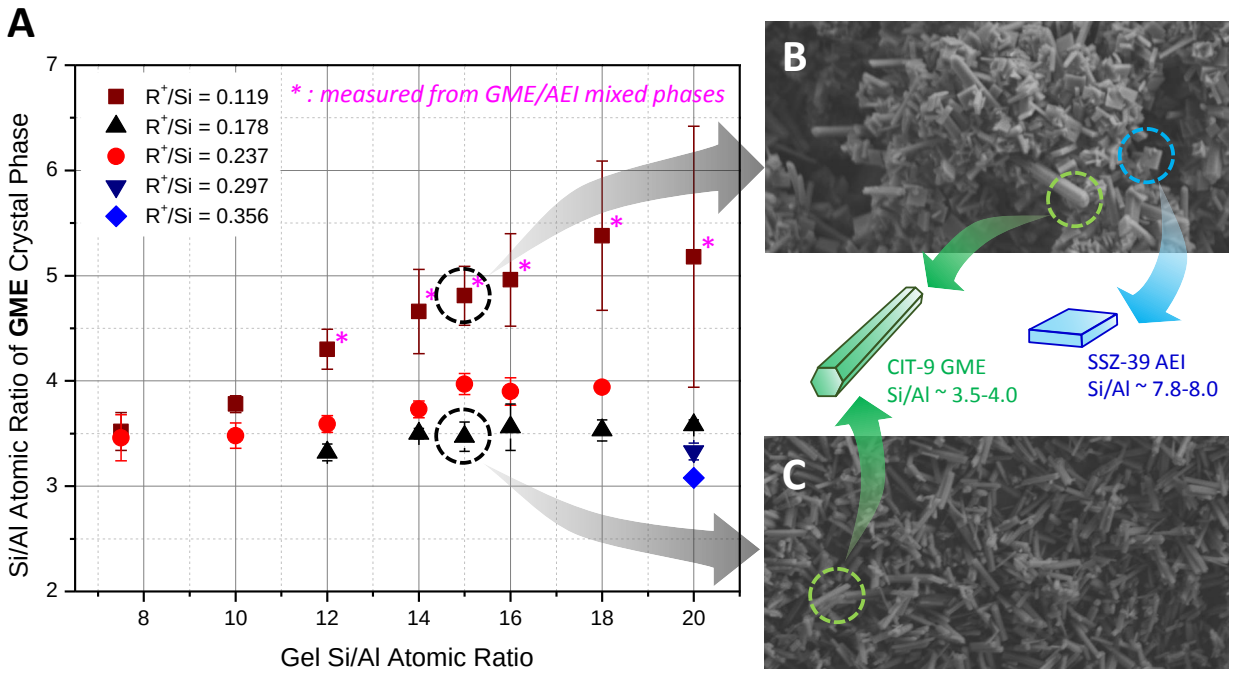

Fig. S2. (A) the empirical relation between the gel Si/Al ratios and those of product crystals. (B-C) the scanning electron micrographs of products obtained from Si/Al = 15 gels with (B) R^+/Si = 0.119 and (C) R^+/Si = 0.178.

Fig. S2A displays the Si/Al ratios of CIT-9 **GME** phase obtained from various gel compositions. Generally, the gels with mid-range OSDA concentration (R/Si = 0.237) resulted in the highest Si/Al ratios of **GME** crystals. At R/Si = 0.237, a synthesis gel with Si/Al = 15 gave **GME** crystal of Si/Al = 3.9-4.0. (This is the highest Si/Al ratio value of all hitherto reported synthetic **GME** materials.) This implies that, other than the aluminum contents of the gels, the concentration of OSDA also plays an important role that determines the elemental composition of resulting **GME** crystals. At a very low concentration of OSDA (R/Si = 0.119), the gels crystallized mixed phases of **GME** and **AEI**. (Figure B) The elemental analyses on these mixed phases were done using an in-built point-ID function of the EDS instrument, and the Si/Al ratios of **GME** and **AEI** phases were separately measured. **GME** crystals in those mixed phases still showed a Si/Al value of approximately 4.0. So we could conclude that Si/Al ~ 4.0 is practically the upper limit of the Si/Al elemental ratio of **GME** zeolites crystallized using N,N-dimethyl-3,5-dimethylpiperidinium hydroxide OSDA.

3.3 Synthesis series used for concentration trend - Figure 1 in main manuscript

This series was synthesized using only different water additions in the mixtures, while keeping Si, Al, Na and OSDA addition, in absolute weights, the same. This was accomplished by using the recipes below, and following procedure in 1.2 for CIT-9. After washing and drying powder, a 2 hour PXRD scan was taken and the relative ratio within one diffractogram of the intensity of the 7.5 degrees 2θ reflection (largest peak reflection of GME structure) over the sum of this intensity and that of the 9.8 degrees 2θ reflection (largest peak reflection of AEI structure) was used to calculate the relative ratio of both phases in the powder and their competition in the synthesis (GME/(AEI+GME)). This is only a tool to estimate the relative occurrence of each phase and not necessarily equals a weight ratio. The ratio found for each concentration is given, along with the synthesis recipe. An enlarged view of Fig. 1 is shown in Fig. S3.

Table S1: Additional information on synthesis with varying concentration of OSDA.

cis-[OSDA]	Molar recipe	GME/(GME+AEI)
0.27 M[a]	**1**SiO_2:**0.066**Al:**0.172**SDA:**0.52**Na^+:**0.69**OH^-:**35**H_2O	pure AEI
0.315 M[a]	**1**SiO_2:**0.066**Al:**0.172**SDA:**0.52**Na^+:**0.69**OH^-:**30**H_2O	0.132
0.34 M[a]	**1**SiO_2:**0.066**Al:**0.172**SDA:**0.52**Na^+:**0.69**OH^-:**27.7**H_2O	0.186
0.36 M[a]	**1**SiO_2:**0.066**Al:**0.172**SDA:**0.52**Na^+:**0.69**OH^-:**26.3**H_2O	0.237
0.37 M[a]	**1**SiO_2:**0.066**Al:**0.172**SDA:**0.52**Na^+:**0.69**OH^-:**25**H_2O	0.186
0.38 M[a]	**1**SiO_2:**0.066**Al:**0.172**SDA:**0.52**Na^+:**0.69**OH^-:**24.8**H_2O	0.382
0.40 M[a]	**1**SiO_2:**0.066**Al:**0.172**SDA:**0.52**Na^+:**0.69**OH^-:**23.6**H_2O	0.498
0.41 M[a]	**1**SiO_2:**0.066**Al:**0.172**SDA:**0.52**Na^+:**0.69**OH^-:**23.0**H_2O	0.575
0.42 M[a]	**1**SiO_2:**0.066**Al:**0.172**SDA:**0.52**Na^+:**0.69**OH^-:**22.5**H_2O	0.522
0.44 M[a]	**1**SiO_2:**0.066**Al:**0.172**SDA:**0.52**Na^+:**0.69**OH^-:**21.5**H_2O	0.786
0.45 M[a]	**1**SiO_2:**0.066**Al:**0.169**SDA:**0.54**Na^+:**0.71**OH^-:**20.7**H_2O	pure GME
0.47 M[a]	**1**SiO_2:**0.066**Al:**0.172**SDA:**0.52**Na^+:**0.69**OH^-:**20**H_2O	pure GME
0.57 M[a]	**1**SiO_2:**0.066**Al:**0.172**SDA:**0.52**Na^+:**0.69**OH^-:**16.5**H_2O	pure GME
0.47 M, racemic OSDA[b]	**1**SiO_2:**0.066**Al:**0.172**SDA:**0.52**Na^+:**0.69**OH^-:**20**H_2O	0.262
0.50 M, Si/Al 30[c]	**1**SiO_2:**0.033**Al:**0.18**SDA:**0.52**Na^+:**0.70**OH^-:**20.4**H_2O	pure GME
0.39 M, Si/Al 30[c]	**1**SiO_2:**0.033**Al:**0.14**SDA:**0.51**Na^+:**0.65**OH^-:**20**H_2O	0.186
0.37 M, Si/Al 30[c]	**1**SiO_2:**0.033**Al:**0.186**SDA:**0.51**Na^+:**0.65**OH^-:**28**H_2O	0.118
0.28 M, Si/Al 30[c]	**1**SiO_2:**0.033**Al:**0.14**SDA:**0.52**Na^+:**0.66**OH^-:**28**H_2O	pure AEI

[a] Static synthesis at 140 °C for 96 hours.
[b] Additionally, a 0.47 M synthesis using racemic OSDA (48 cis / 52 trans; see section 1.1) was run in exactly the same conditions. The PXRD of this spectrum is found in Fig. 1.
[c] Static synthesis at 140 °C for 2-5 days.

The first 13 rows of this table are found in **Fig. 1B**. Further data, for a series with Si/Al 30 in the mixture, confirm the trend. E.g. the '0.37 M, Si/Al 30' entry shows that adding more OSDA relative to the Si, Al and Na content (vs. 0.28 M, Si/Al 30 experiment) does not suffice to get pure GME: at the same time, the H_2O content needs to be taken down as well, to surpass 0.47M and generate

pure GME (= 0.50 M, Si/Al 30 synthesis). The opposite, taking down water, but keeping OSDA/Si at 0.14 (as in 0.28 M experiment), also does not yield pure GME. Although OSDA concentration is likely the key factor, it cannot be excluded that the OH^--concentration also has an effect as more OSDA and less water always heightens the OH^--concentration as well. Using the OSDA in its Br^--form could possibly answer this question, if devoid of bromine interfering.

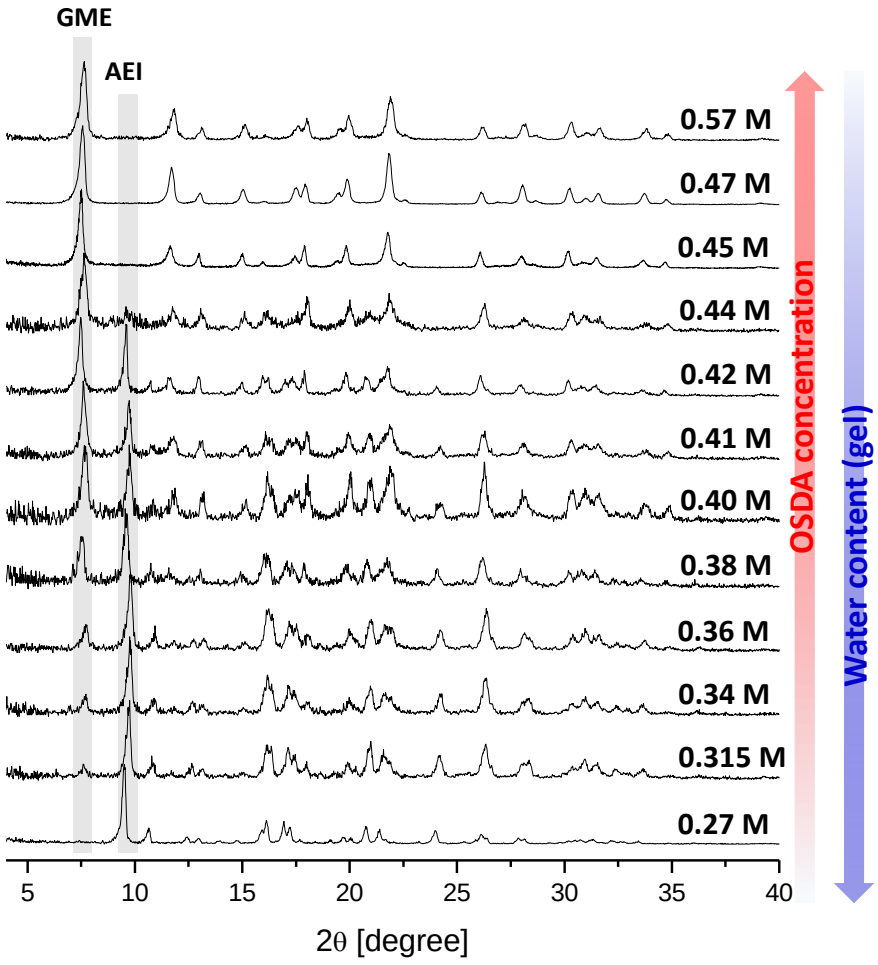

Fig. S3. Series with small variation in recipe and switch between AEI (lower trace) and GME (upper trace): water content and inversely, OSDA concentration. (larger version of Fig. 1 inset)

3.4 Effects of Si/Al ratios of the starting material zeolite Y.

Table S2: Additional information on synthesis with various zeolite Y as the starting material.

#	Source Y	cis-[OSDA], gel Si/Al*	Molar recipe	Results
1	CBV712	0.48 M, Si/Al 28	**1**SiO_2:**0.035**Al:**0.170**SDA:**0.50**Na^+:**0.67**OH^-:**19.4**H_2O	pure AEI[b]
2	CBV720	0.48 M, Si/Al 66	**1**SiO_2:**0.015**Al:**0.167**SDA:**0.50**Na^+:**0.66**OH^-:**19.0**H_2O	pure AEI[a]
3	CBV760	0.48 M, Si/Al 129	**1**SiO_2:**0.008**Al:**0.165**SDA:**0.49**Na^+:**0.66**OH^-:**18.8**H_2O	pure AEI[a]
4	CBV712	0.45 M, Si/Al 6	**1**SiO_2:**0.167**Al:**0.200**SDA:**0.50**Na^+:**0.70**OH^-:**15**H_2O	pure GME[a]
5	CBV712	0.71 M, Si/Al 12	**1**SiO_2:**0.083**Al:**0.200**SDA:**0.50**Na^+:**0.70**OH^-:**15**H_2O	pure GME[a]
6	CBV720	0.68 M, Si/Al 15	**1**SiO_2:**0.067**Al:**0.200**SDA:**0.50**Na^+:**0.70**OH^-:**15**H_2O	pure GME[a]
7	CBV720	1.4 M, Si/Al 15	**1**SiO_2:**0.067**Al:**0.400**SDA:**0.30**Na^+:**0.70**OH^-:**15**H_2O	Dense Phase[b]
8	CBV720	0.71 M, Si/Al 30	**1**SiO_2:**0.033**Al:**0.200**SDA:**0.50**Na^+:**0.70**OH^-:**15**H_2O	AEI+Dense[b]
9	CBV720	1.4 M, Si/Al 30	**1**SiO_2:**0.033**Al:**0.400**SDA:**0.30**Na^+:**0.70**OH^-:**15**H_2O	No transformation[b]

* When Si/Al of gel differs from starting FAU, Si was added in form of Sodium silicate. [a] Static synthesis at 140 °C for 96 hours (4 days).
[b] Static synthesis at 140 °C for 240 hours (10 days).

In an attempt to obtain higher Si/Al GME, different Y-zeolites, used as Al and (partial) Si-source in these syntheses, have been tested. The classic recipe uses CBV500 with **Si/Al 2.6**. Table S2 show the results of crystallizations when higher silica USY materials were used instead of CBV500 as the Al-source for hydrothermal crystallization, i.e. CBV712 (**Si/Al = 6**), CBV720 (**Si/Al = 15**), and CBV760 (**Si/Al = 30**).

As long as the overall gel compositions remained within the CIT-9 chemistry range, pure GME phases were crystallized. (Trial #**4-6**) On the other hand, the increased gel Si/Al ratios due to low Al-contents of the starting zeolite Y (simple replacement in weight of CBV500 in original recipe) resulted in the crystallization of AEI phases instead of desired GME phases, (Trials #**1-3**, #**8**) which is compatible with the other examples shown in this work.

The Si/Al ratios of CIT-9 GME obtained from higher silica USY (CBV712 and 720) were 2.96 (#**4**), 3.59 (#**5**), and 3.66 (#**6**) despite the low Al-contents of higher silica USY zeolites. This implies the crystallization of GME is not governed a lot by the Si/Al ratios of starting Y-zeolites but more by the overall gel compositions. #4 and #6 are noteworthy since pure GME phases could be obtained without using any other additional Si-source such as sodium silicate; *i.e.*, in these batches, USY zeolites exclusively provided both Si and Al for crystallization of GME. This might be relevant in terms of simplifying the synthesis procedure (e.g. ref [8]).

No transformation of Y to either GME or AEI was observed when a higher R^+/Na^+ ratio was employed. (#**7, 9**) The XRD profiles of the Trial #1-9 are provided in the following Fig. S4.

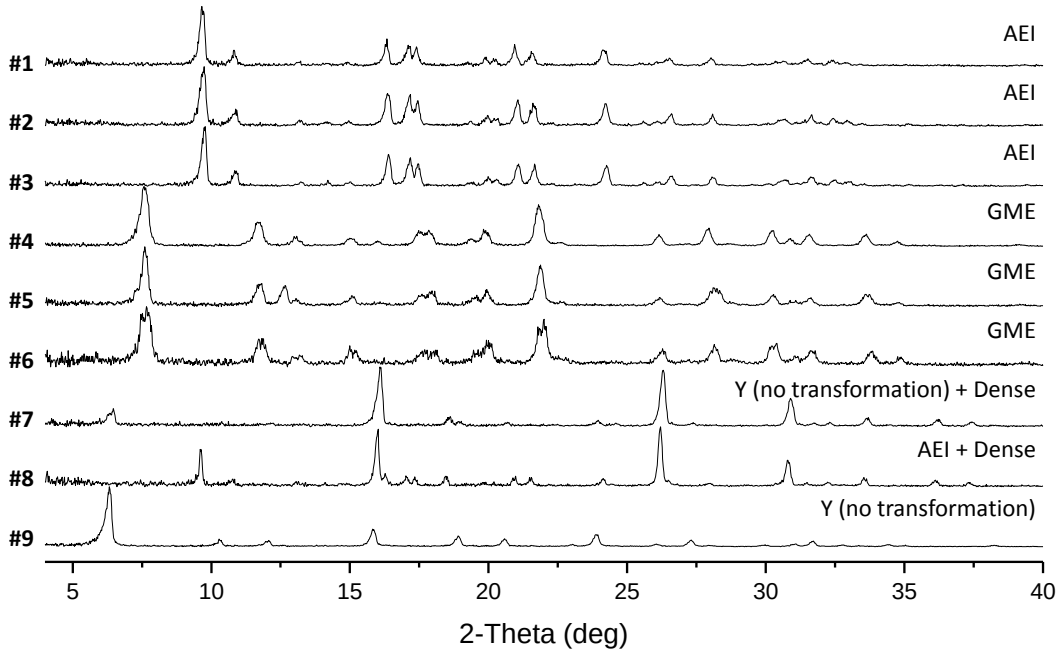

Fig. S4. PXRD patterns of syntheses series with variation in the source Y-zeolite, Table S2.

3.5 Molecular modelling images (molecular mechanics simulations) of cis vs trans

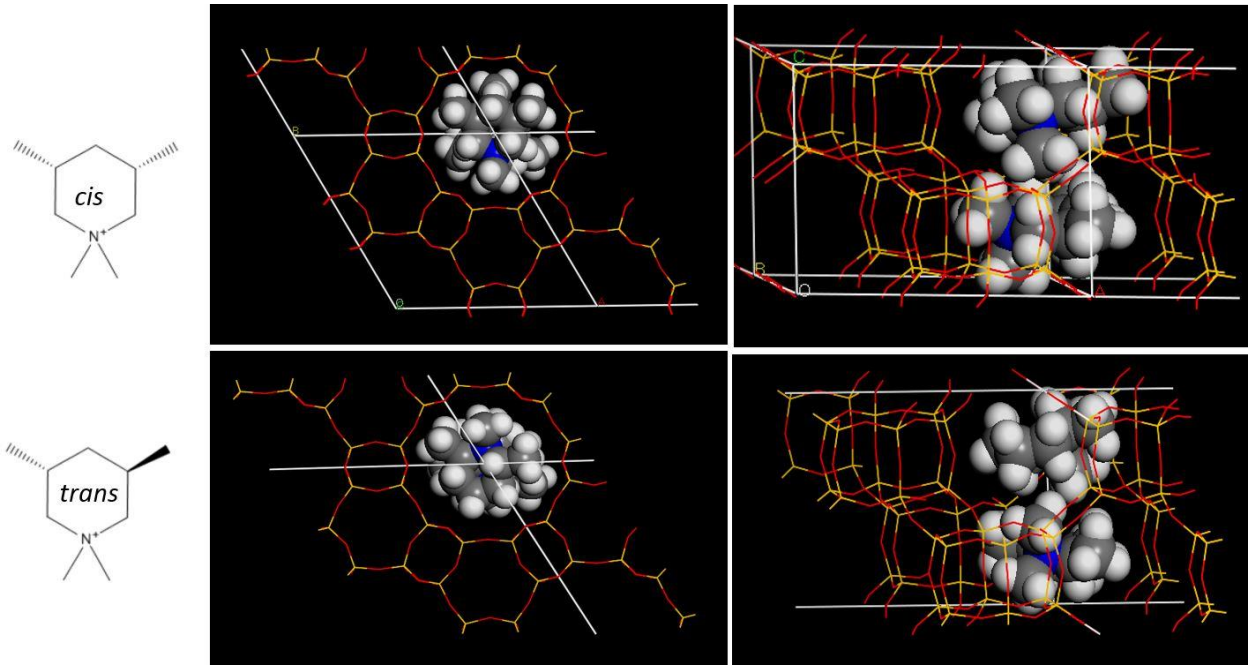

Fig. S5. Perfect 'rosette' fit between 2 ***cis***-tetramethyl-N,N,3,5-piperidinium cations (up) and the GME 12 MR. On the right, 2 OSDAs are seen per unit cell. The ***trans*** fit (down) is clearly less tight.

3.6 ^{13}C CP-MAS NMR of OSDA inside CIT-9

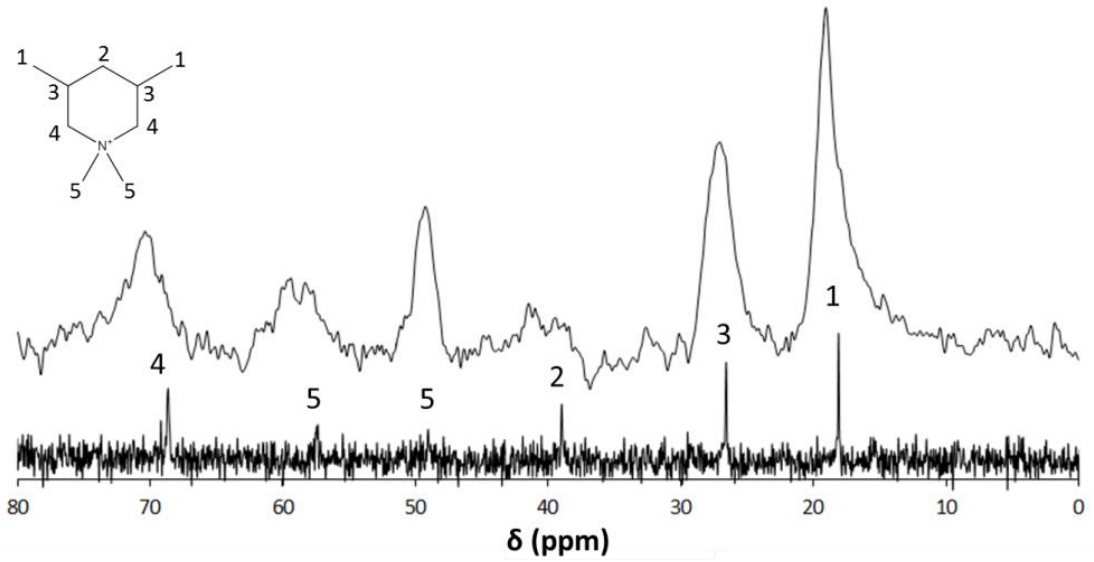

Fig. S6. ^{13}C CP MAS NMR analysis of as-made CIT-9 (upper trace) and the OSDA cis-tetramethyl-N,N,3,5-piperidinium hydroxide standard (lower trace), 500 Mhz.

The occluded OSDA is clearly intact. This CP MAS NMR technique allows to distinguish cis from trans isomers of this OSDA, inside pore (here only cis used and found) as demonstrated in ref. [1]

3.7 TGA data with OSDA/unit cell estimation of CIT-9

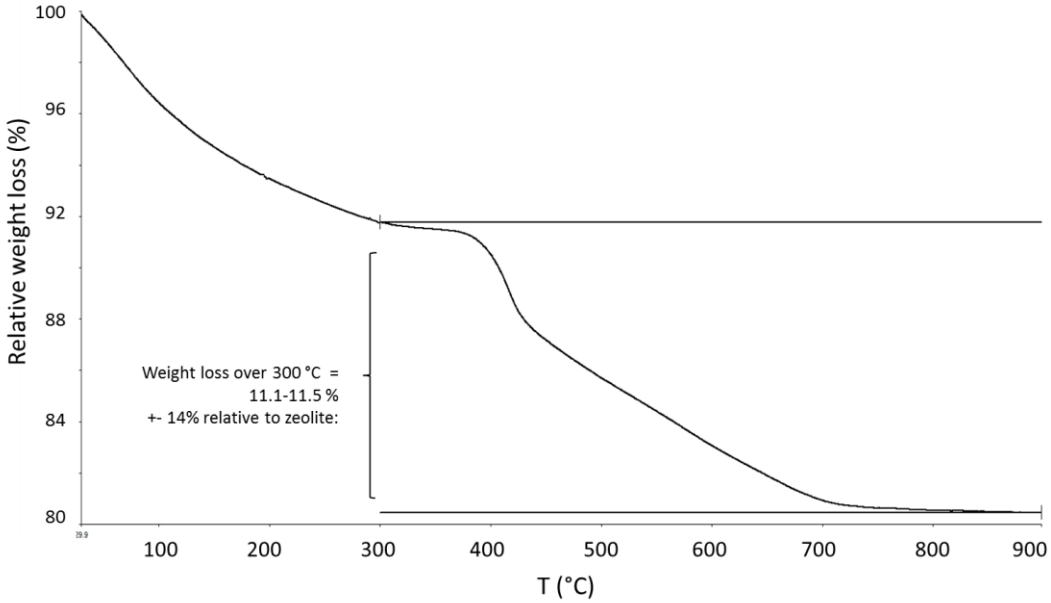

Fig. S7. Thermogravimetric analysis of an as made CIT-9.

Thermogravimetric analysis of a typical air-dry as-made material shows that the total weight loss equals about 20%. The weight loss fraction over 300 °C is attributed to the removal of the OSDA

and a good measure for the amount of its incorporation. Relative to the Na-containing zeolite left at 900 °C, the included amount of OSDA was found to be around 14 wt%, converting to 1.5 OSDA molecules per unit cell. This calculation is based on estimating the weight of a perfect, dry, organic-free unit cell containing 24 T-atoms (4.8 Al,19.2 Si or Si/Al = 4), 48 oxygens and 3.3 Na^+ cations (from Na/Al in EDS and also from iteration until $(Na+OSDA)^+/Al = 1$) and taking this as representative for what is left at 900 °C in TGA. The organic weight fraction relative to that can be divided by the molecular weight of the OSDA cation. This calculation (1.5 OSDA / u.c) is prone to (severe) underestimation, e.g. if a small organic-free amorphous aluminosilicate phase is present or full crystallinity is not achieved (washing removes excess, not-occluded OSDA).

Since GME is a 1D-12MR, and the organic is too large to fit in the 8MR channels or subunit gme-cages, the TGA results confirm that the OSDA stabilizes the 12MR channel. Per unit cell, the length of the 12MR channel is about 1 nm, while the OSDA has a diameter of about 0.5-0.6 nm.[3] The modelling results showed best stabilization energies for two OSDAs per unit cell Considering this is an idealized scenario, that does not considers defects, possible faulting and surface terminated imperfect unit cells (all lowering actual OSDA incorporation), TGA is in fair agreement with the model. Anyway, the trans-OSDA modeling energies were consistently lower than the cis-values for the same occupations.

3.8 Characterization of dabco-GME

Dabco-GME synthesis is very tedious and a lot of optimization was needed to be able to obtain pure GME according to a modified recipe based on Kerr et al. (see section 1.2). dabco-GME was characterized with SEM/EDS (Table S4, Fig. S9), PXRD (Fig. S15), RED (Fig. S10), N2-physisorption (Table S3), TGA (below) and solid state NMR (Fig. S20). The main reason to produce dabco-GME was to be able to make a fair comparison for our new CIT-9 material with the best reported one, using the latest techniques to assess faulting and disorders.

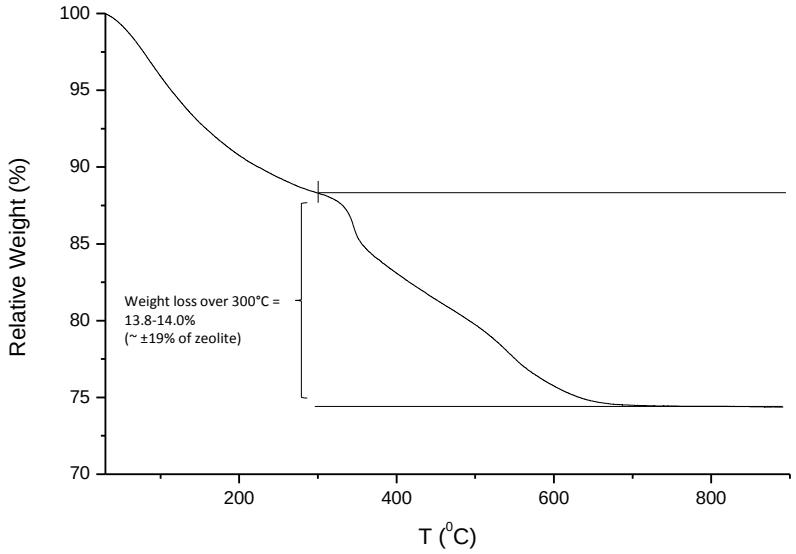

Fig. S8. Thermogravimetric analysis of an as made dabco-GME.

3.9 SEM images comparing CIT-9 and dabco-GME

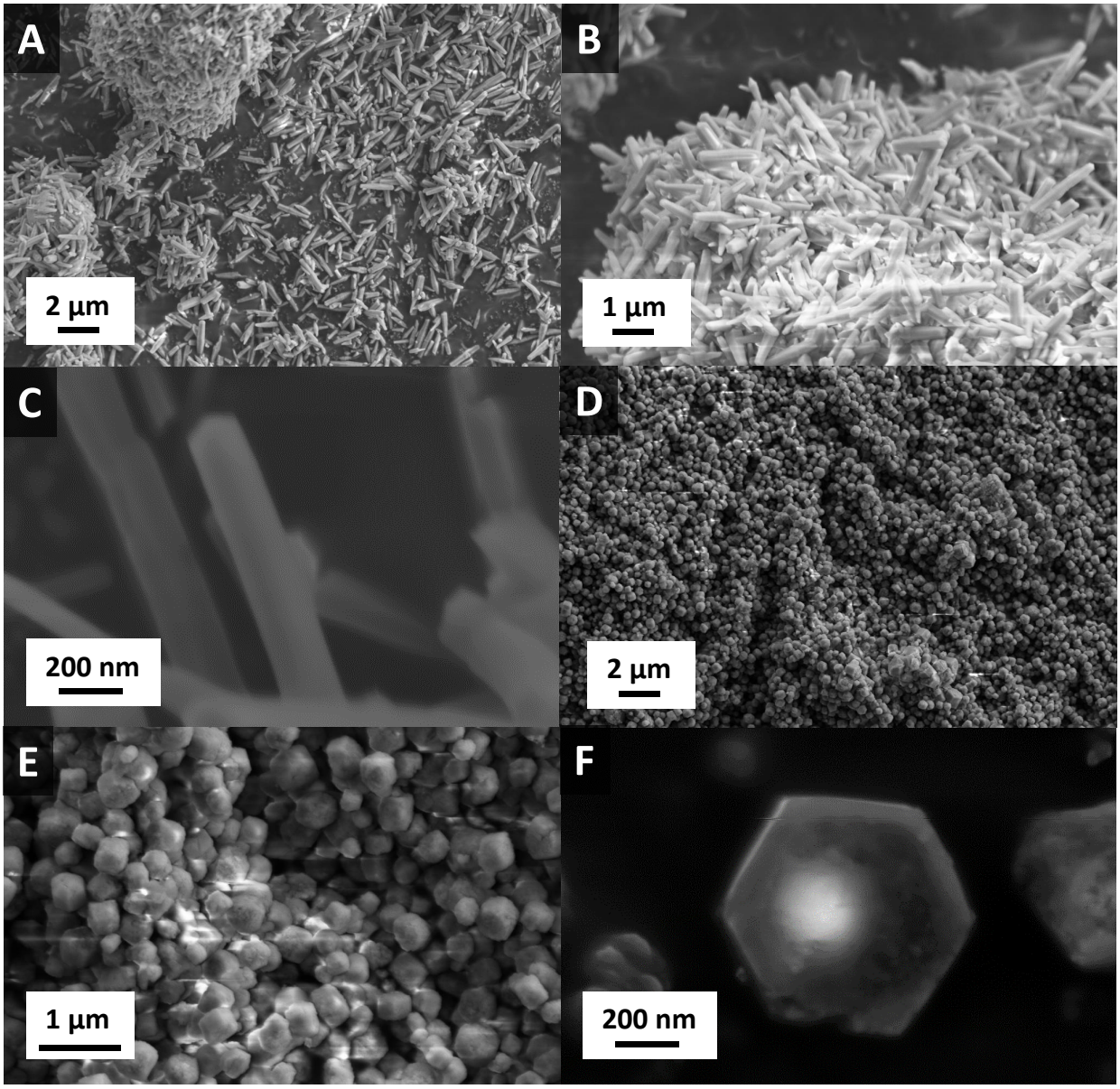

Fig. S9. SEM-images of A-C) as made CIT-9 and D-F) dabco GME

3.10. Rotation electron diffraction data

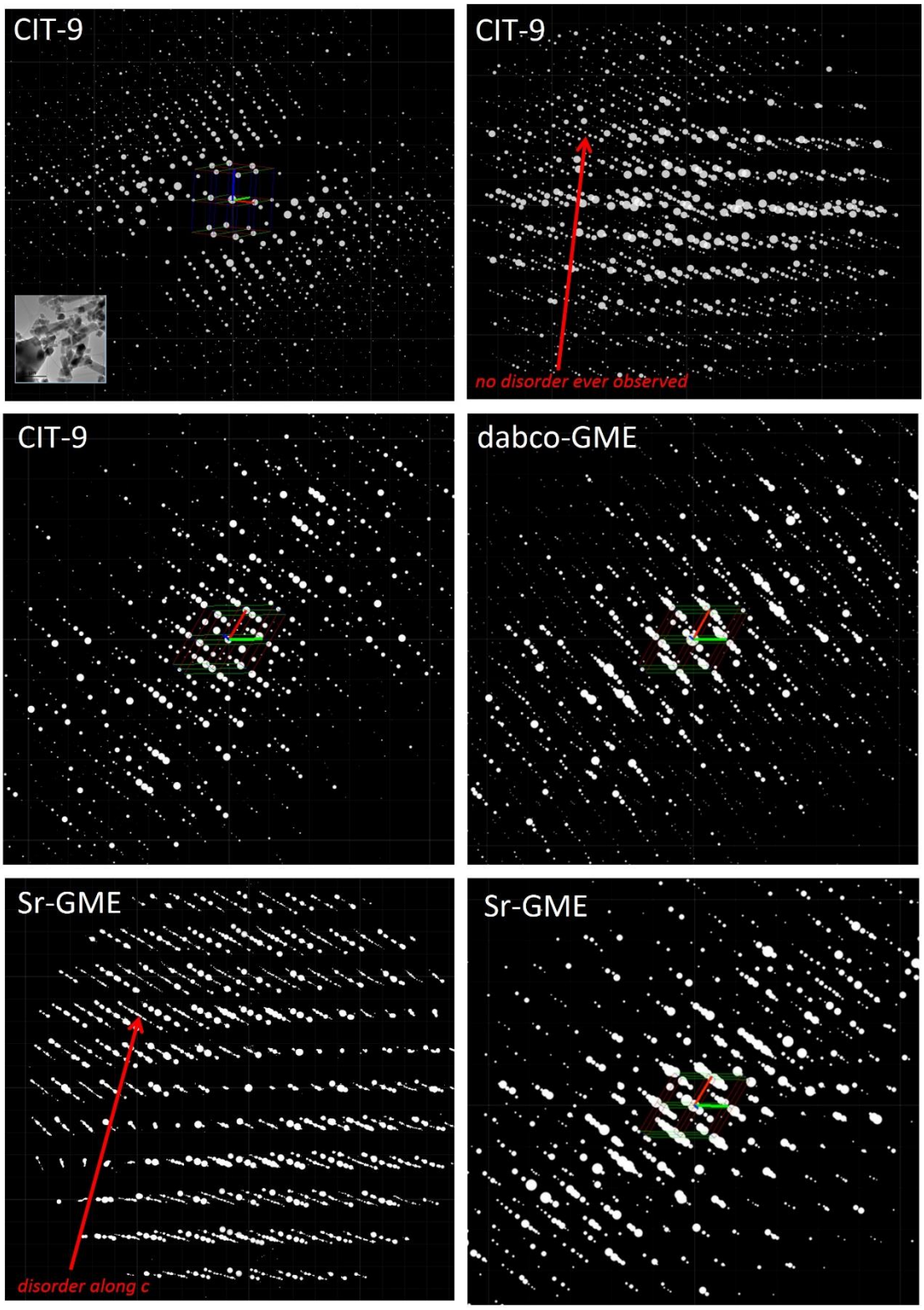

Fig. S10. Additional RED images for CIT-9, Sr-GME and dabco-GME. The ones with a unit cell indicated, are looking down in the c-axis (blue), except upper left. a,b axes are green and red.

3.11 Comparison of PXRD of CIT-9 and other GME materials in PXRD and Si/Al ratio

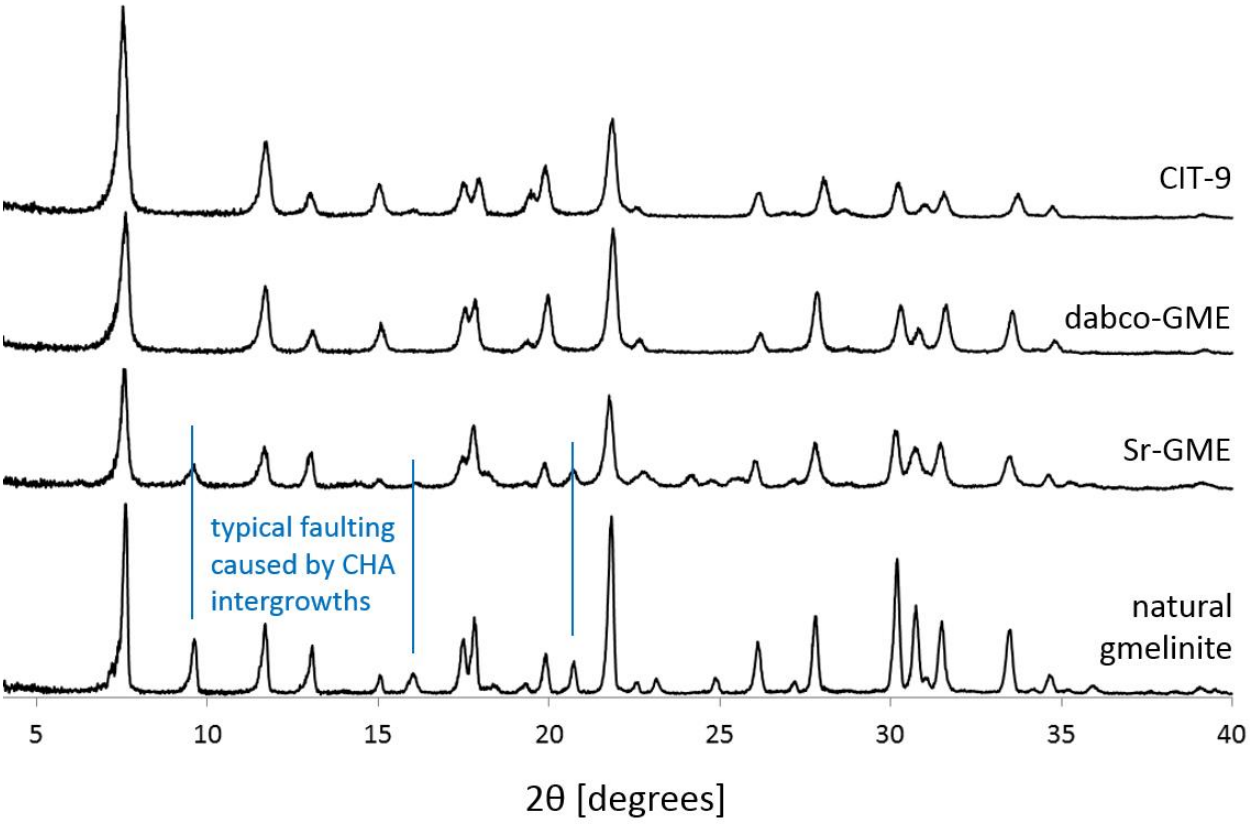

Fig. S11. Comparison of PXRD patterns of the different known GMEs. Sr-GME was measured in its Na^+-from (sample from Chiyoda) as dabco-GME, CIT-9 and natural gmelinite also contain Na^+.

3.12 Thermal behavior of CIT-9: Variable Temperature XRD study

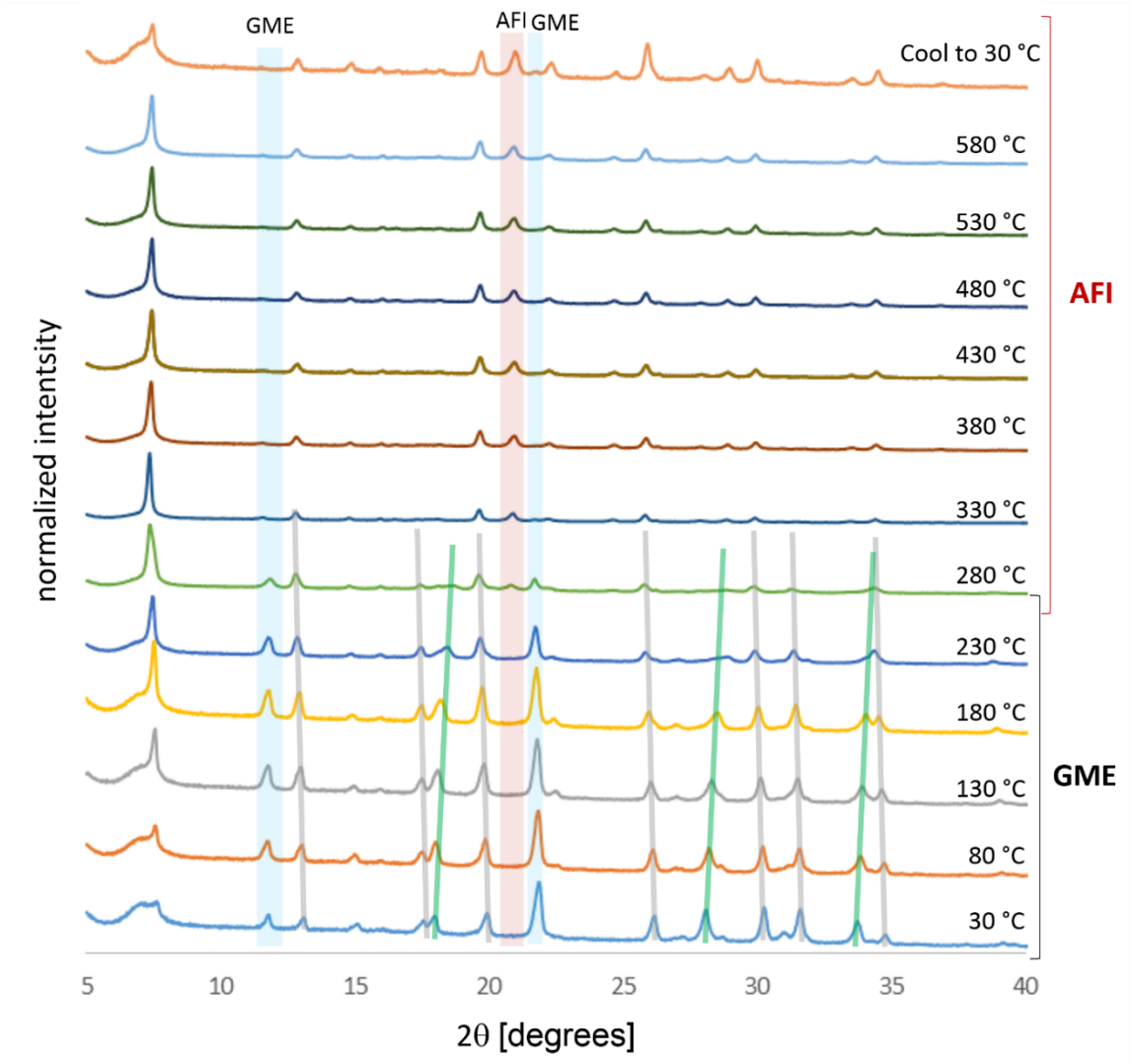

Fig. S12. Full normalized (not scaled as in Fig. 4) variable-temperature XRD dataset of CIT-9.

Key reflections of GME are shifting right (green) or left (grey), indicating either a,b axis expansion or c-axis shrinking. This is already seen from 80 °C onwards, and up to 280 °C. At 330 °C (and beyond range) GME has already transformed to AFI. Some reflections of GME fully disappear (blue), some new AFI reflections appear (red). Both topologies share the 7.5 degrees 2θ reflection. Some AFI reflections are already apparent in the 280 °C diffractogram, indicating the transformation roughly occurs around 300 °C. This is in line with Alberti et al. seeing a gmelinite mineral turn into AFI type material at 300 °C.[9]

The 100 reflection at 7.5 degrees 2θ at low temperature is broadened due to the instrument and OSDA presence. The oxidation (in situ calcination) of the OSDA renders this peak sharper. The classic Rigaku 25°C data show an intense sharp peak and normal shape.

3.13 N_2-physisorption study

Table S3. Micropore volumes of GME samples from t-plot on adsorption branch

Type of GME	Treatment	Micropore volume[a] cm^3/g (Micromeritics)	Micropore volume[b] cm^3/g (Quantachrome)
CIT-9	ozone-treated	0.17[c]	0.175
	ozone + K-exchange	0.11	0.095
	ozone + K-exchange + calcination	0.15	0.14
	special KCl calcination	0.15	0.15
dabco-GME	ozone-treated	0.12[c]	0.12[d]
	ozone + K-exchange	0.13	n.d.
	ozone + K-exchange + calcination	0.09	n.d.
Sr-GME	data from ref.[4], Na^+-form	0.03	n.a.
gmelinite	data from ref.[4]	0.02	n.a.

[a] Often average of 2 measurements on Micromeritics TriStar II (pretreated at (200 °C + N_2-flow overnight). [b] Quantachrome Autosorb iQ (vacuum degassing using slow T-ramp up to 200 °C, 6h). [c] Note that ozone-treated samples are in partial Na^+,H^+ form. [d] physically different sample than in Micromeritics measurements, but from an exact batch reproduction synthesis. CIT-9 and dabco-GME values from one sample series.

To ensure maximum data accuracy and reproducibility of the T-sensitive GME, multiple adsorption experiments were run. Ozone-treated samples showed the loss of the organic fraction by ozone and took up +-15-17 wt% of water.

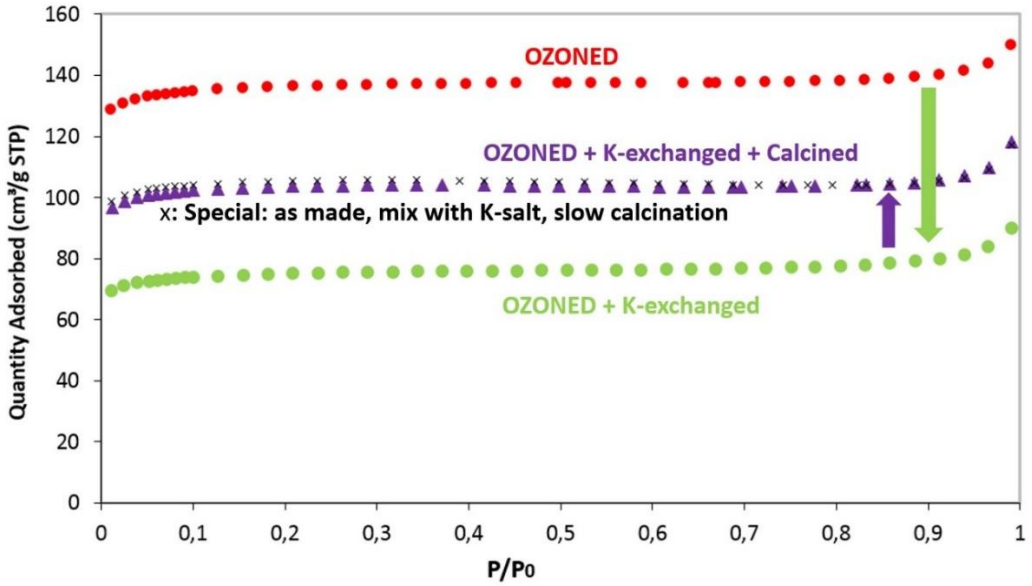

Fig. S13. CIT-9 physisorption isotherms after different treatments (PXRD, viz. Fig. S14).

3.14 Thermal behavior of CIT-9 and dabco-GME: Ozone-treatment and K^+-exchange

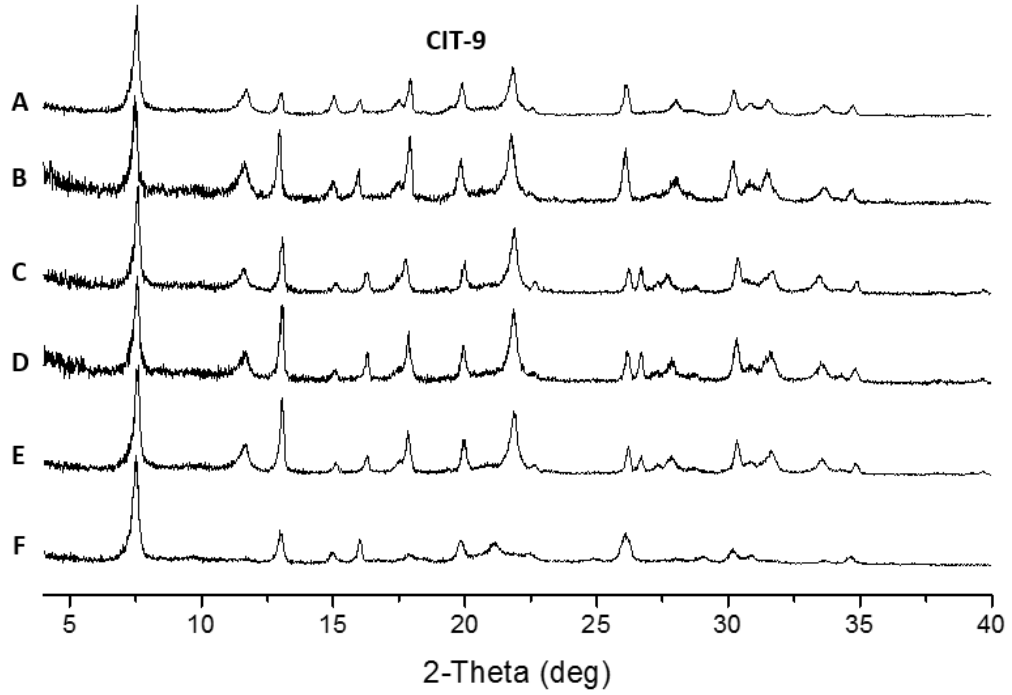

Fig. S14. CIT-9 diffractograms after different thermal and ion-exchange treatments. **A** = as-prepared; **B** = ozoned; **C** = ozoned + K-exchanged (Kx); **D** = ozone + Kx + calcined; **E** = special K-mix calcination; **F**: (AFI) direct calcination of as-made.

The thermal behavior of CIT-9 (as-made trace A), with transformation to AFI in absence of K (trace F); and its preserved framework and good pore volume after ozone treatment (B) is followed in PXRD patterns. K-exchanging the ozone-treated materials (C) allows them to be stable and survive high-T calcination (trace D, prevents AFI formation). A slow calcination of a special high concentrated KCl-slurry with as-made CIT-9 allows to prevent AFI as well, and remove the OSDA at once (E). This is explained under sections 3.15 with method from section 1.4.

Likewise, prepared dabco-GME samples undergo the potassium cation-exchange to preserve the GME framework after ozone-treatment. Figs. S15A, B and C show the powder XRD profiles of as-prepared, ozone-treated, and K^+-exchanged forms of dabco-GME materials. The framework of this potassium-exchanged GME survived the calcination treatment at 580°C for 6 hours without transformation to AFI (trace D). Without this potassium exchange step, as-prepared dabco-GME was transformed to AFI after the same calcination step (Fig. S15F). Fig. S15E.

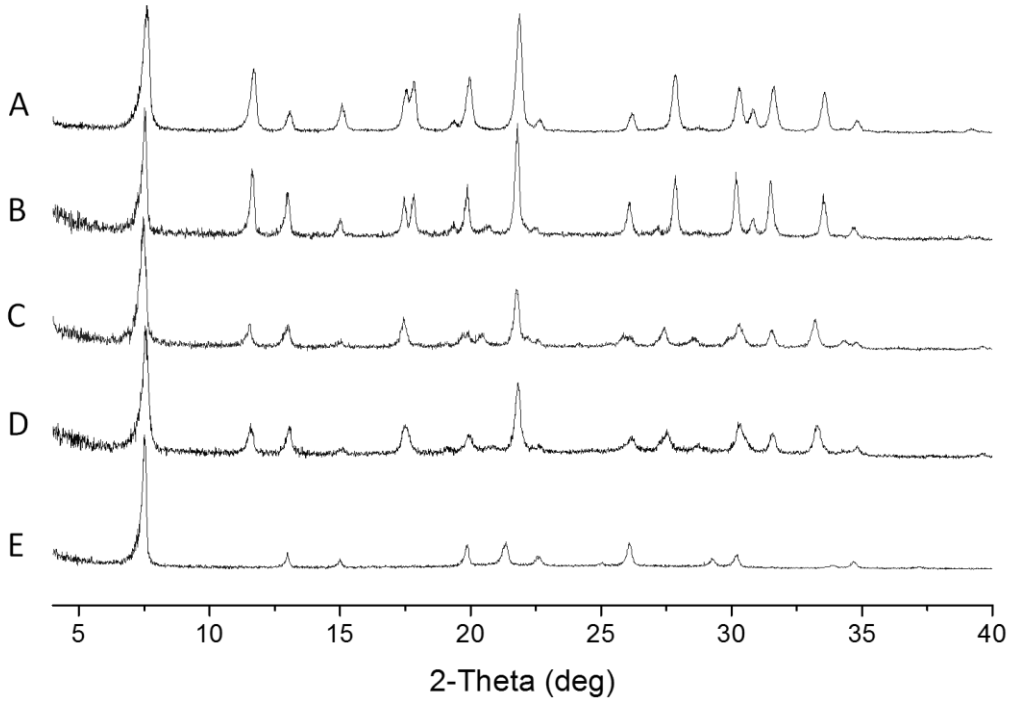

Fig. S15. XRD profiles of dabco-GMEs, with same legends for A-E as in Fig. S14.

Dabco-GME, long thought to be fault-free based on a sorption experiment[3], was in fact measured after calcination in that work, which in absence of K^+, now shows AFI was likely probed instead of GME.

3.15 Thermal behavior of CIT-9 and dabco-GME: slurry K-salt-mix calcination method

Interestingly, a patent[5a] was found in literature describing the stabilization of dabco-GME during calcination for organic removal by adding excess salts and slow heating. This procedure was tried both for CIT-9 and dabco-GME and indeed proved to work: a careful slurry of concentrated salt (see section 1.4) was prepared. Using 100% KCl, stabilization of GME reflections was found, while not AFI peaks appeared. Using mixtures of KCl and NaCl salts and even pure NaCl in the case of CIT-9 allowed this treatment to work. However, after removal of excess extra-framework salt followed by re-calcination in normal conditions did not stop the GME from changing into AFI in the presence of Na^+ alone. K^+ is thus clearly needed for the void-framework to survive 580 °C. K likely occupies positions in 8MR windows, or perhaps, even in the *gme* cavity. The latter would sure make sense since the GME-AFI transformation involves the compressing of these cavities (see Fig. 4).

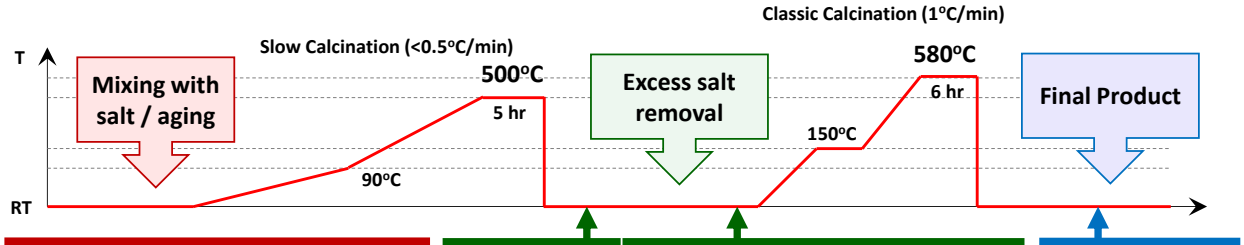

Sample Code Mixed-salt composition (mol%)	Phase after 1st calc.	Framework (K^+ : Na^+) Atomic Ratio (EDS)	Phase after 2nd calc.
CIT-9 (Crystal Si/Al = 3.9-4.0)	**CIT-9**		**CIT-9**
KCl 100%	**GME**	K 85% : Na 15%	**GME**
KCl 75% : NaCl 25%	**GME**	K 78% : Na 22%	**GME**
KCl 50% : NaCl 50%	**GME**	K 66% : Na 34%	**GME**
KCl 25% : NaCl 75%	**GME**	K 31% : Na 69%	**GME+AFI**
NaCl 100%	**GME**	Na 100%	**AFI**
(No Salt)	**AFI**		
DABCO GME (Crystal Si/Al = 2.7-2.8)	**DABCO GME**		**DABCO GME**
KCl 100%	**GME**	K 87% : Na 13%	**GME**
KCl 75% : NaCl 25%	**GME**	K 74% : Na 26%	**GME**
KCl 50% : NaCl 50%	**GME**	K 56% : Na 44%	**GME+AFI**
KCl 25% : NaCl 75%	**GME**	K 30% : Na 70%	**AFI**
NaCl 100%	**GME+AFI**	Na 100%	**AFI**
(No Salt)	**AFI**		

Fig. S16. Excess salt-mix treatment-calcination explained and tested on CIT-9 and dabco-GME.

Table S4. Different existing GMEs compared to CIT-9

Type of GME	Si/Al	Faulted? Disorder?	Reference
CIT-9	3.5 – 4.0	None in RED	*This work*
dabco-GME	2.7 – 2.8 (3.5)*	A little, from RED	self-made* and[10]
Sr-GME	2	A lot, Visible in XRD, RED	Chiyoda, Davis[4]
Natural gmelinite	2.18	A lot, visible in XRD, RED	Chiyoda, Davis[4]

*Kerr[3] reported a range of 2.6 to 3.5 for dabco-GME. Huo reported 2.3.[5a]

3.16 Solid state MAS NMR of CIT-9 and other GME materials

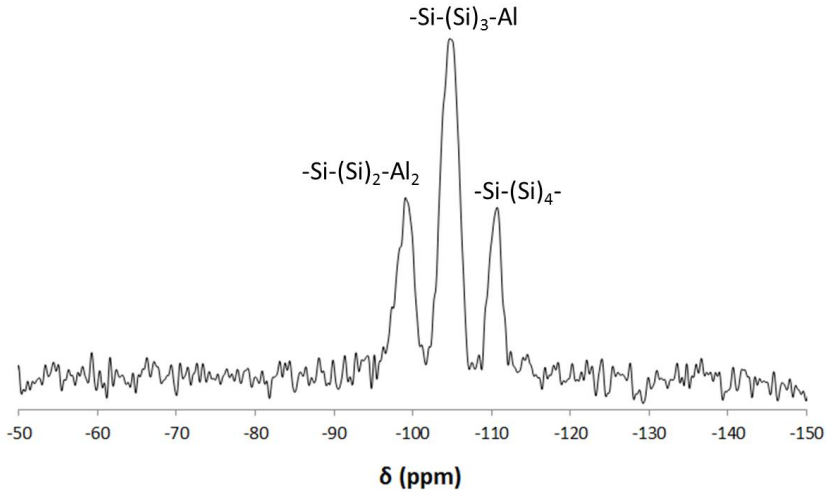

Fig. S17. ^{29}Si MAS NMR of CIT-9 after ozone-treatment, K-exchange and calcination at 580 °C.

Three characteristic signals of typical aluminosilicates with intermediate-high Al content are seen in Fig. S17. The intensities of these resonances at -98 ppm (2Al), 105 ppm (1Al) and 110 ppm (0Al) allow to calculate the Si/Al ratio according to the known formula.[11] This leads to a Si/Al value of 3.9, well in accord with a value of 4.0 for this CIT-9 sample in EDS. Fig. S18 compares this spectra to known spectra for GMEs from literature. The high Si/Al ratio of the new CIT-9, is reflected in the distribution of signals versus the other lower Si/Al state of the art GME materials (less 0Al). Also worth noting is the absence of -94 ppm signal in CIT-9 while present in all other GME materials. This signal is indicative of Si surrounded by 3Al or some aluminums and defect silanols.

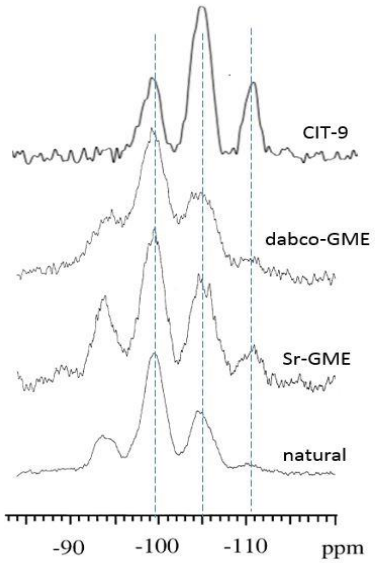

Fig. S18. ^{29}Si MAS NMR of CIT-9 (ozone, K-exchanged, calcined) on top of 3 spectra from literature for dabco-GME, Sr-GME and natural gmelinite (adapted from Chiyoda and Davis[4]).

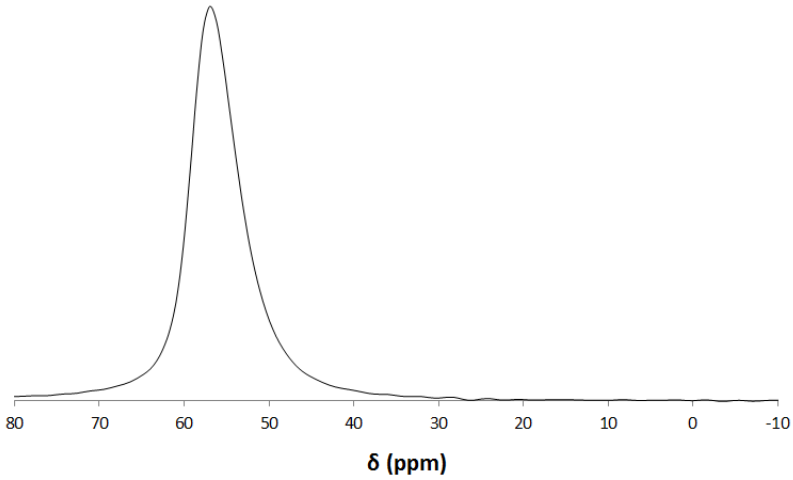

Fig. S19. ^{27}Al MAS NMR of CIT-9 after ozone treatment, K-exchange and calcination at 580 °C

The absence of signals at 0 ppm in Fig. S19 and S20 (right) and the presence of the large signal at 57 ppm show that all Al is incorporated tetrahedrally into the GME framework in CIT-9.

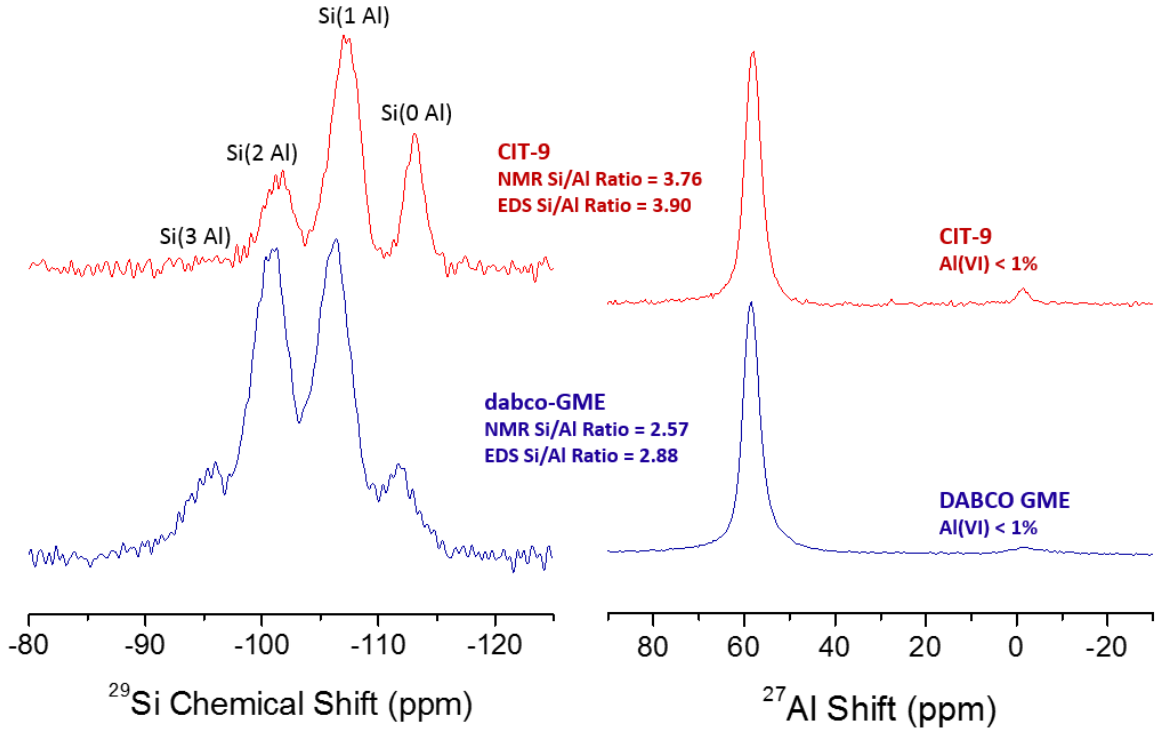

Fig. S20 Comparison of ozone-treated GME in ^{29}Si MAS NMR (left) and ^{27}Al MAS NMR (right) for CIT-9 and home-made dabco-GME.

The Si/Al of these samples measured via the formula and bulk via EDS is shown in the series. Again, the Si/Al of CIT-9 is higher than that of dabco-GME.

3.17 Steam-treatment of K-exchanged CIT-9 GME.

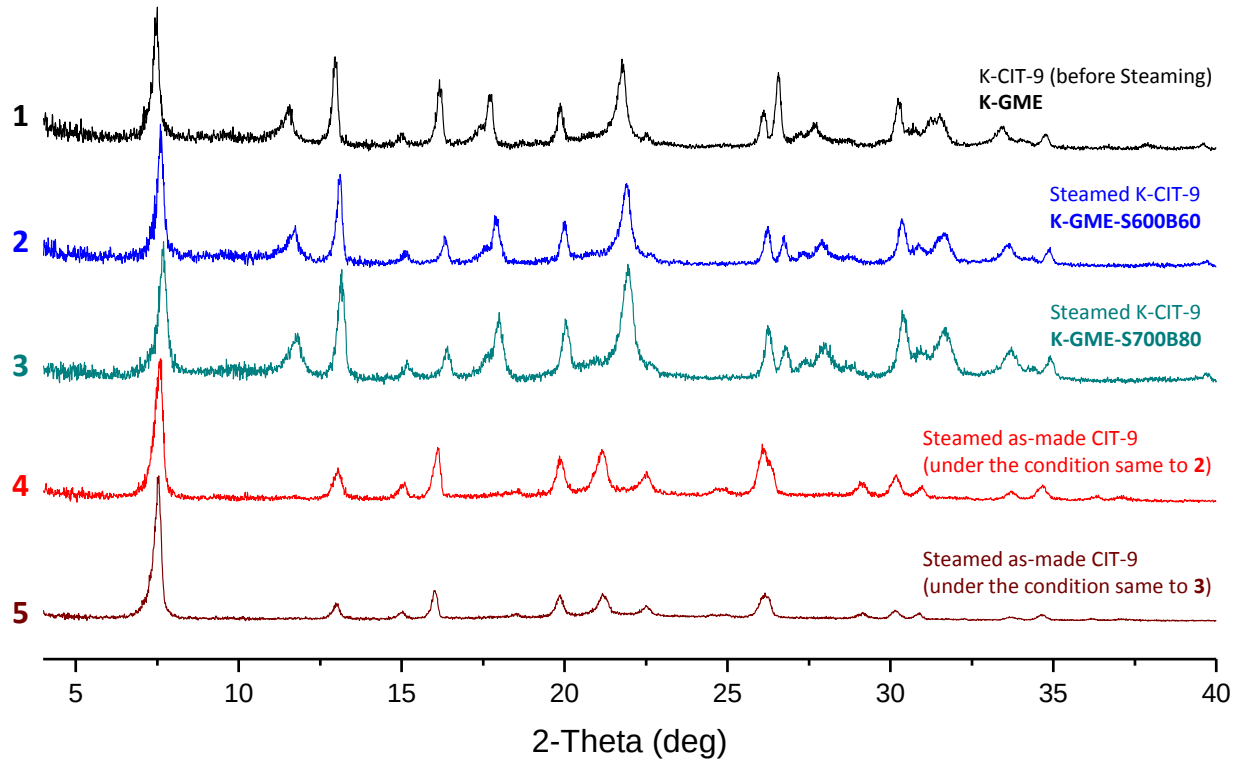

Fig. S21. XRD profiles of CIT-9 before and after two different steaming treatments: K-exchanged CIT-9 GME before steaming (**1**), steamed K-CIT-9 GME (**2, 3**), and steamed as-made CIT-9 (**4, 5**). The latter two in absence of K^+ are converted to AFI-framework.

The steaming of K-exchanged CIT-9 GME was studied. A batch of typical K-CIT-9 was steamed under two conditions: furnace temperature of 600 °C with bubbler temperature of 60 °C (steam partial pressure = 20 kPa) and furnace temperature of 700 °C with bubbler temperature of 80 °C (steam partial pressure = 47 kPa). The steamed products were named K-GME-S600B60 and K-GME-S700B80, respectively. All steaming treatments were performed for 6 hours. Fig. S21 shows the framework of K-exchanged CIT-9 GME survived steaming conditions without degradation. (profile **1, 2, 3**) Meanwhile, under the same conditions, as-made CIT-9 GME samples without K-exchange were completely transformed into AFI frameworks. (profile **4, 5**) This proves that the presence of potassium ions within framework is essential for CIT-9 GME to survive not only high-temperature calcination conditions but also steaming processes.

It is noteworthy that the position of XRD peak corresponding to GME-(100) diffraction has been shifted from 7.50° to 7.60° (K-GME-S600B60) and 7.69° (K-GME-S700B80), respectively, implying the shrinkage of frameworks. We believe that slight dealumination by steaming is responsible for this decrease in the unit cell parameter.

The steamed K-exchanged CIT-9 GME samples were subjected to solid-state ^{29}Si NMR to characterize the elemental composition of silica-based tetrahedral frameworks (Fig. S22) The mild and harsher steaming processes resulted in small but reproducible increases in $Si/Al_{(Tetrahedral)}$ ratios of K-CIT-9. Although the effects of dealumination via steaming of the K-form of CIT-9 were

not large compared to those seen in the steaming of NH_4-exchanged small-pore zeolites[6, 12], this result definitely displays the possibility of modifying CIT-9 GME zeolites via hydrothermal post-synthetic methods, for further catalytic purposes based on the K-stability.

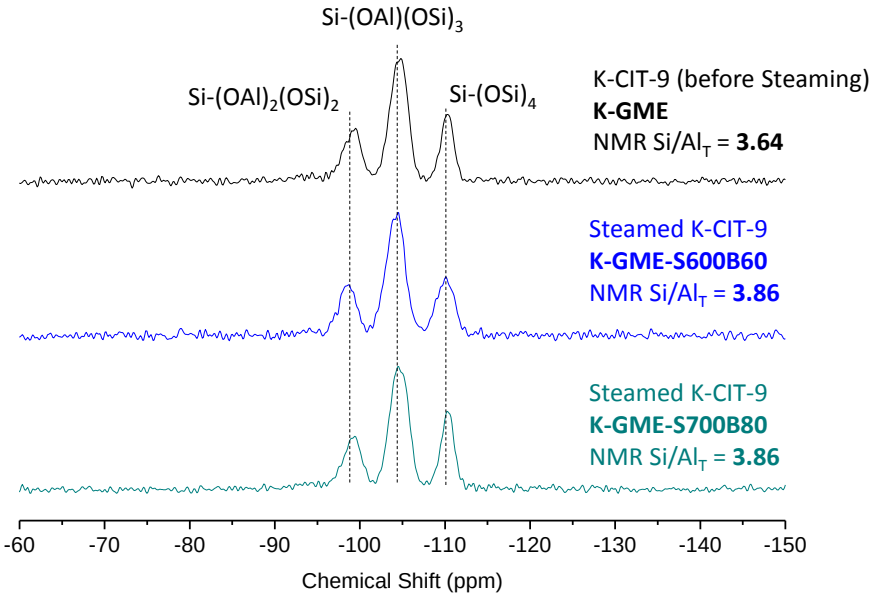

Fig. S22. ^{29}Si NMR spectra of K-exchanged CIT-9 GME before and after steaming processes.

4. References

[1] M. Dusselier, J. E. Schmidt, R. Moulton, B. Haymore, M. Hellums, M. E. Davis, *Chem. Mater.* **2015**, *27*, 2695-2702.

[2] T. Takewaki, L. W. Beck, M. E. Davis, *Microporous Mesoporous Mater.* **1999**, *33*, 197-207.

[3] R. H. Daniels, G. T. Kerr, L. D. Rollmann, *J. Am. Chem. Soc.* **1978**, *100*, 3097-3100.

[4] O. Chiyoda, M. E. Davis, *Microporous Mesoporous Mater.* **2000**, *38*, 143-149.

[5] aQ. Huo, *United States Pat.*, US6423295, 2002; bQ. Huo, N. A. Stephenson, *United States Pat.*, US6632767 2003.

[6] M. Dusselier, M. A. Deimund, J. E. Schmidt, M. E. Davis, *ACS Catal.* **2015**, *5*, 6078-6085.

[7] D. Zhang, P. Oleynikov, S. Hovmöller, X. Zou, in *Zeitschrift für Kristallographie International journal for structural, physical, and chemical aspects of crystalline materials, Vol. 225*, **2010**, p. 94.

[8] N. Martin, C. R. Boruntea, M. Moliner, A. Corma, *Chem. Commun.* **2015**, *51*, 11030-11033.

[9] A. Alberti, I. Parodi, G. Cruciani, M. C. Dalconi, A. Martucci, *Am. Mineral.* **2010**, *95*, 1773-1782.

[10] M. E. Davis, C. Saldarriaga, *J. Chem. Soc., Chem. Commun.* **1988**, 920-921.

[11] H. van Bekkum, E. M. Flanigen, P. A. Jacobs, J. C. Jansen, Elsevier, **2001**.

[12] aY. Ji, J. Birmingham, M. A. Deimund, S. K. Brand, M. E. Davis, *Microporous Mesoporous Mater.* **2016**, *232*, 126-137; bM. A. Deimund, L. Harrison, J. D. Lunn, Y. Liu, A. Malek, R. Shayib, M. E. Davis, *ACS Catal.* **2016**, *6*, 542-550; cY. Ji, M. A. Deimund, Y. Bhawe, M. E. Davis, *ACS Catal.* **2015**, *5*, 4456-4465.